ALTERNATIVE SHOCK CHARACTERIZATIONS FOR CONSISTENT SHOCK TEST SPECIFICATION*

Thomas J. Baca
Sandia National Laboratories
Albuquerque, New Mexico

Mechanical shock environments must be characterized in the most complete manner possible if they are to be successfully simulated in the shock test laboratory. The objective of the research described in this paper is to evaluate three methods of analyzing transient acceleration time histories which represent promising alternatives to shock response spectra as the basis for deriving consistent shock test specifications. A shock test specification is defined to be consistent if it meaningfully relates the operational and laboratory shock environments. The limitations of shock spectra are discussed in this regard before presenting the advantages of the new alternative characterizations. These shock analysis techniques include: 1) ranked peaks in the acceleration time history; 2) root-mean-square acceleration as a function of time; and 3) root-mean-square acceleration as a function of frequency. These shock characterizations provide the parameters necessary to develop a new shock test specification technique which can replace the current practice of enveloping shock spectra. Data from a simulated field shock environment are analyzed using all three shock characterizations as well as shock spectra. The new method of shock test specification is demonstrated using drop table and decaying sinusoid shock test inputs. Test specifications using the standard method of shock spectra enveloping are also derived. The resulting shock test specifications are compared and the implications of using alternative shock characterizations in deriving consistent test specifications are identified. Beneficial aspects of utilizing these alternative shock analysis techniques instead of shock spectra are presented with particular emphasis being placed on the evaluation of conservatism associated with different shock test specification techniques.

INTRODUCTION

Shock tests are specified to simulate operational shock environments. Aerospace components are shock tested in the laboratory to develop confidence that they will survive the flight shock environment. The adequacy of the shock test as a consistent substitute for the field shock can only be judged if both shock environments are characterized properly. Shock spectra are currently used in the aerospace industry to characterize shock environments and to subsequently specify shock tests. A shock test input is taken to be acceptable if its shock spectrum envelops the shock spectrum of the field data. The objective of this paper is to develop an alternative to shock spectrum enveloping for shock test specification. The proposed method of shock test specification requires a more complete characterization of both laboratory and field shock data. This method requires calculation of root-mean-square acceleration as a function of frequency and time, as well as the sorting of peak acceleration values in the shock time history. This new test specification technique is implemented for decaying sinusoid and and haversine shock test inputs which are two widely used types of laboratory excitation. A comparison of this method with the standard shock spectrum approach will finally be undertaken through a study of both the test inputs and analytically derived responses from a simple structure.

*This work was supported by the United States Department of Energy.

LIMITATIONS OF SHOCK SPECTRA IN DERIVING CONSISTENT SHOCK TEST SPECIFICATIONS

A discussion of the limitations of using shock spectrum enveloping as the sole means of specifying shock tests is useful in motivating the development of a test specification technique based on alternative shock characterizations. An absolute acceleration shock spectrum (SAA) is a plot of the maximum value of the absolute acceleration response of a single degree of freedom system (SDOF) having a specified critical damping ratio versus the natural frequency of the SDOF system. The concept of shock spectra was conceived by Biot [1,2] as a means of characterizing the strong ground motion of earthquakes by their effects on simple SDOF models of buildings. The key aspect of the shock spectrum is that it reflects the effects of a transient on a certain class of structures (i.e., SDOF structures with a certain damping ratio). It does not retain information about the specific characteristics of the shock. In spite of this intended use of the shock spectrum concept, shock spectra are widely used in the aerospace community as an acceptable means of characterizing a shock environment [3]. Shock test specification has been implemented through the selection of laboratory test inputs having shock spectra which exceed the shock spectra of available field data [4]. Objections to this procedure have been raised previously [5-8], particularly in the context of assessing shock test conservatism [6-8]. The principal reason for the acceptance of shock spectrum enveloping as a test specification technique is that component structures which can survive tests specified in this manner, generally perform well in the operational shock environment.

The implications of shock spectrum enveloping can be demonstrated through the following example. Consider the shock time history shown in Figure 1a which was measured as the input to the fixed end of a 12.7 cm (5 inch) long metal cantilever beam mounted in a support structure. Given that this is the operational shock environment, what kind of test pulse should be applied in the shock laboratory? The most common answer would be the 1300 g x 0.33ms haversine pulse shown in Figure 1b.

A haversine pulse is defined by the following equation:

$$\ddot{x}(t) = \begin{cases} \frac{A}{2}\left(1 - \cos\frac{2\pi t}{TH}\right), & 0 < t < TH \\ 0 & \text{elsewhere} \end{cases} \qquad (1)$$

where A is the amplitude of the haversine pulse and TH is the duration. These haversine pulse parameters are derived by selecting the haversine pulse having a shock spectrum that envelops the shock spectrum of the field data, as shown in Figure 2.

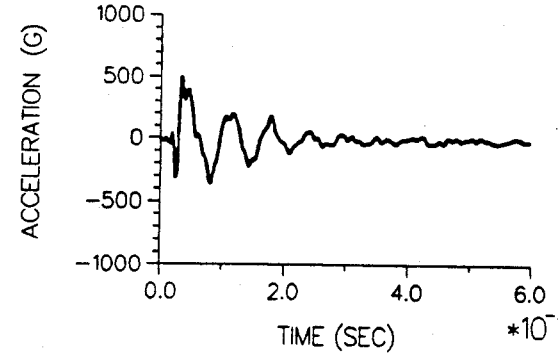

Figure 1a Time History for Field Data.

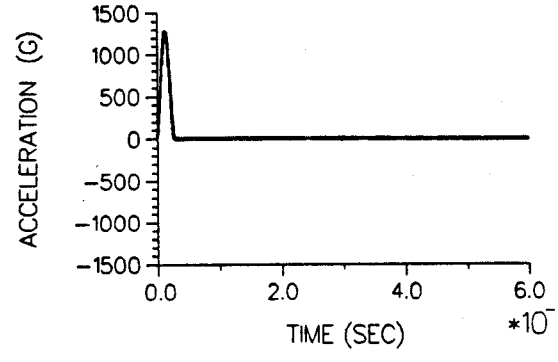

Figure 1b Time History for 1300 g x 0.33 ms Haversine Shock Test Specification.

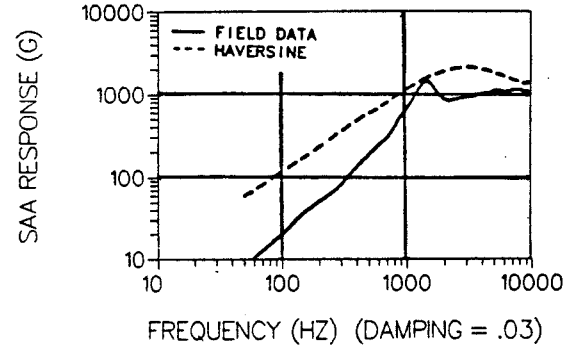

Figure 2 Comparison of Shock Spectra for Field Data and 1300 g x 0.33 ms Haversine Shock Data.

While the main advantage of the haversine pulse is that it can be created repeatedly on a drop table shock machine, the obvious disadvantage is that it does not resemble the field shock data in terms of its peak acceleration, two-sidedness, or duration. These observations can be made by an inspection of the time histories in Figures 1a and 1b. Since the shock spectrum (Figure 2) is not a measure of frequency content, it is necessary to look at a comparison of the energy spectra (Fourier amplitude spectrum squared) to see that the two shock excitations vary markedly in terms of frequency content (see Figure 3). One final approach to evaluating these two shock pulses is to calculate the response at the end of a finite element model of the beam when it is excited by each pulse. The results of this calculation performed using MSC/NASTRAN are shown in Figures 4a and 4b. A much higher response is produced by the haversine pulse than by the field data pulse.

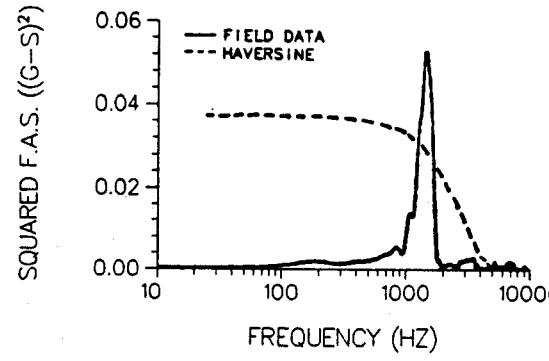

Figure 3 Comparison of Squared Fourier Amplitude Spectra for Field Data and 1300 g x 0.33 ms Haversine Shock.

ALTERNATE SHOCK CHARACTERIZATIONS

The alternative shock characterizations to shock spectra employed in this paper were originally introduced as significant descriptors of field and laboratory shock environments which could be used to meaningfully quantify and actually control shock test conservatism [6,8]. These characteristics of shock transients aim to describe the distinctive features of a particular shock environment so that these same characteristics will be preserved in a laboratory test shock pulse. Consequently, these alternative shock characterizations are unlike the shock spectrum which quantifies only the effects of a shock on SDOF structures.

Three main characteristics of the shock time history have been preserved in the alternative shock characterizations:

1) the variation of the average amplitude of the acceleration time history as a function of time,

2) the frequency content of the shock excitation,

3) the magnitude of the peaks in the acceleration time history.

Time domain root-mean-square acceleration, TRMS (τ), is defined as a measure of the first of these characteristics:

$$TRMS(\tau) = \left[\frac{1}{\tau} \int_0^{\tau} \ddot{x}^2(t)dt \right]^{1/2}$$

$$0 < \tau \leq TD \qquad (2)$$

where TD is the duration of the shock transient.

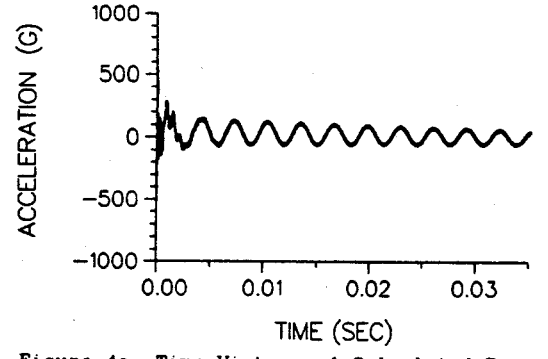

Figure 4a Time History of Calculated Response at End of Cantilever Beam to Field Data Input (Figure 1).

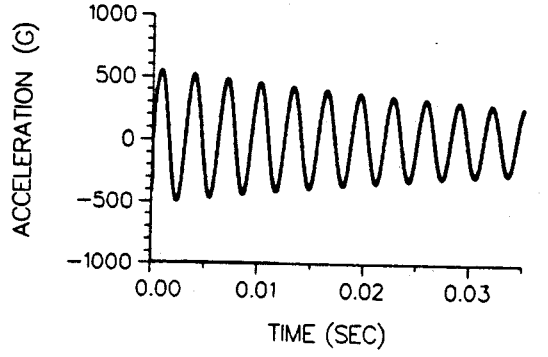

Figure 4b Time History of Calculated Response at End of Cantilever Beam to 1300 g x 0.33 ms Haversine Shock Input (Figure 2).

At time τ = TD, the overall RMS acceleration for the time history, TRMSO, is an overall indicator of the average acceleration level experienced during the shock event. It is important to remember that each TRMSO value must have a duration, TD, associated with it to be meaningful. Overall TRMS values from two different shock events must have the same analysis duration before any comparison can be made between the two time histories. A plot of TRMS versus time for the field data time history in Figure 1 is shown in Figure 5.

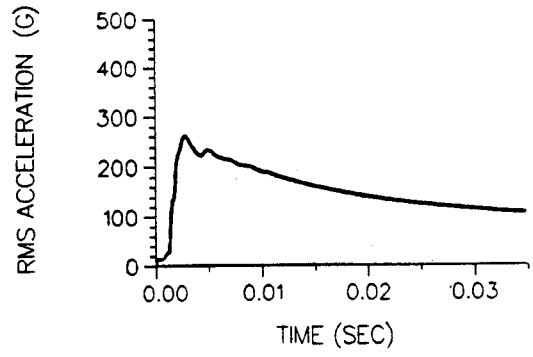

Figure 5 Time Domain RMS for Field Data (Figure 1).

It was shown previously [6] that the contribution to the overall TRMS acceleration (TRMSO) by all frequencies less than the frequency of interest F is given by a frequency domain RMS acceleration:

$$FRMS(F) \cong \frac{2}{TD}\left[\int_0^F |\ddot{X}(f)|^2 df\right]^{1/2} \qquad (3)$$

where $\ddot{X}(f)$ is the Fourier transform of $\ddot{x}(t)$:

$$\ddot{X}(f) = \int_{-\infty}^{\infty} \ddot{x}(t)\, e^{-j2\pi ft} dt \qquad (4)$$

and $j = \sqrt{-1}$.

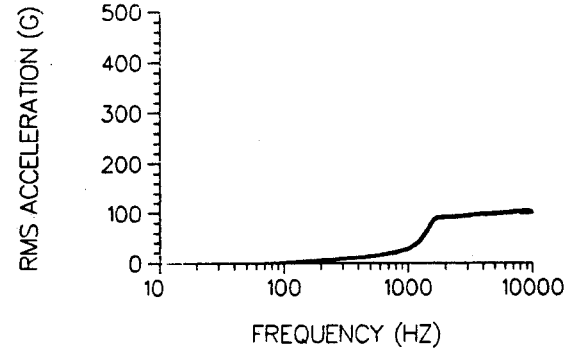

Figure 6 Frequency Domain RMS for Field Data (Figure 1).

Figure 6 shows a plot of FRMS for the field data shock (Figure 1). Note that a sharp increase in the FRMS level is indicative of substantial frequency content at that frequency (e.g., ~1500 Hz in Figure 6). The FRMS plot has the advantage over the Fourier amplitude spectrum that it not only reflects frequency content, but also retains a readily interpretable numerical value. The numerical value at a given frequency of the Fourier amplitude spectrum is not as directly amenable to physical interpretation. It should again be emphasized that the FRMS plots of two shocks can only be compared if they both have a duration equal to TD. Keeping track of the duration of a transient helps to retain an important characteristic of the shock time history. (No more effort is involved than that of specifying the critical damping ratio associated with a particular shock spectrum.) Finally, calculation of FRMS is accomplished efficiently. Fast Fourier Transform techniques [9] allow the rapid solution of Equation (4), while the integration specified in Equation (3) can be accomplished numerically.

An acceleration peak is defined to be the maximum value between changes in sign of the time history. Once positive and negative peaks have been identified, a sorting algorithm [6] can be applied to rank: all of the peak values; the positive peak values; and the negative peak values. The ranked peak accelerations for all peaks in the field data time history in Figure 1 are shown in Figure 7. This plot serves as a summary of the extreme acceleration values of the shock time history. Plotting the positive

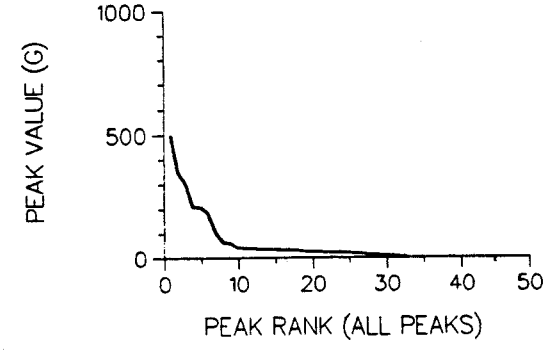

Figure 7 Ranking of Absolute Peaks for Field Data (Figure 1).

and negative ranked peaks on the same curve (see Figure 8) provides valuable insight into the two-sidedness of the shock time history. Comparisons of ranked peaks from two time histories should be done only if both records have been filtered to ensure that each will have the same bounds on their frequency content.

ALTERNATIVE SHOCK TEST SPECIFICATION METHOD

It is important to emphasize that a complete understanding of a shock excitation requires study of all three of the alternative shock characterizations. The goal of consistent shock test specification is to match the shock characterizations of the field data and the laboratory test shock input to the greatest extent possible. Knowledge of the failure mechanisms of the structure being tested may be of use in judging the significance of each of the shock characterizations, but the approach taken in this paper is to consider each of them to be equally important. It is also assumed that the time histories of the field shock data are available to the engineer responsible for shock test specification. The three parameters used in the proposed shock test specification require calculation of the overall RMS acceleration (TRMSO), FRMS(F), and the maximum peak acceleration. Normally, it would be expected that all of the shock characterizations previously mentioned would have been determined for the field data.

Test specification procedures are given in the following paragraphs for decaying sinusoid and haversine shock test inputs. A decaying sinusoid shock pulse is composed of a sum of decaying sinusoids of the form:

$$\ddot{x}(t) = \begin{cases} Ae^{-2\pi tZ/T}\sin\frac{2\pi t}{T}, & t \geq 0 \\ 0, & t < 0 \end{cases} \qquad (5)$$

Methods exist for specifying decaying sinusoid shock test inputs on the basis of enveloping shock spectra [10]. The intuitively attractive feature of the decaying sinusoid pulse is that it allows the shock input to be more "realistic looking" when one is attempting to simulate pyrotechnic shocks which are two-sided, decaying types of shocks (e.g., Figure 1). The main restriction on the use of the decaying sinusoid shock pulses is that they are limited to the force capability of the shaker system on which they are implemented. Haversine shock test inputs (as given by Equation (1)) are commonly generated on drop table shock machines. This test technique has the advantage of being able to achieve higher peak acceleration levels than those of decaying sinusoid pulses produced on shakers. The widespread use of haversine shock test inputs motivates development of a test specification technique for these simple pulses in this paper.

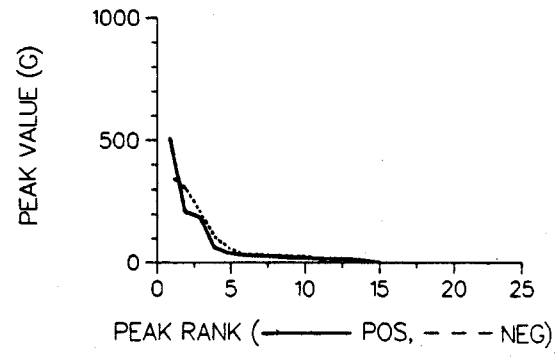

Figure 8 Ranking of Positive and Negative Peaks for Field Data (Figure 1).

The parameters of interest in the test specification processes discussed next are as follows:

- Z = Decay rate of the exponential term in the decaying sinusoid component
- A = Amplitude of decaying sinusoid or haversine pulse
- T = Period of decaying sinusoid component (T=1/f, where f is the frequency of the sinusoid)
- TH = Baseline duration of the haversine pulse
- TD = Analysis duration of both field shock and test shock
- TP = Time for the exponential factor in the decaying sinusoid to decay to P percent of its original amplitude
- TRMSO = Overall RMS acceleration for duration TD.

Decaying Sinusoid Test Specification:

Selecting an appropriate decaying sinusoid shock requires that values of A, Z, and T be selected for each frequency which is judged to be significant in the FRMS plot. The procedure described here is for a single component, but the method applies to any number of decaying sinusoid components. (Note that a low frequency and low amplitude compensating pulse [10] must be included to make the shock pulse have zero final velocity and displacement.)

The value of T is first selected by looking at a plot of FRMS for the field data. The predominant frequency of the field data will be indicated by a sharp increase in slope in the FRMS plot. More than one frequency may be evident in the field data, so that more decaying sinusoid frequency components may be needed. The contribution to the overall TRMSO value of each predominant frequency can be measured from the FRMS plot as well.

Observation of the field shock data will yield the time at which the shock has decreased

to P percent of its peak level. Defining the ratio of TP to T as:

$$RP = \frac{TP}{T} \qquad (6)$$

the value of P is controlled by the exponential decay rate, Z:

$$P = 100 \cdot (e^{-Z2\pi \cdot RP}) \qquad (7)$$

so that in general,

$$RP = \frac{-1}{2\pi Z} \ln \left(\frac{P}{100} \right) \qquad (8)$$

Figure 9 shows plots of Equation (8) for P=1,2,10,20. These curves can be used to select a value of Z which will give approximately the same effective duration of the shock for a decaying sinusoid component having period T.

Once Z is selected, a value of A is sought based on the TRMSO value. This can be accomplished in a general way by first defining a normalized duration for the decaying sinusoid pulse:

$$R = \frac{TD}{T} \qquad (9)$$

Solving Equation (2) in terms of R for a decaying sinusoid as defined in Equation (5) gives a normalized TRMSO:

$$\frac{TRMSO(R)}{A} = \frac{1}{\sqrt{8\pi R}} \left[\left(\frac{1}{Z} - \frac{Z}{Z^2+1} \right) + e^{-4\pi ZR} \left(\frac{1}{Z} + \frac{\sin 4\pi R - Z \cos 4\pi R}{Z^2 + 1} \right) \right]^{1/2}$$

$$, R > 0. \qquad (10)$$

This equation is plotted in Figure 10 for several damping values. Knowing the desired TRMSO value, Z, and R for the field data, A can be found once the value of TRMSO(R)/A is determined from Figure 10.

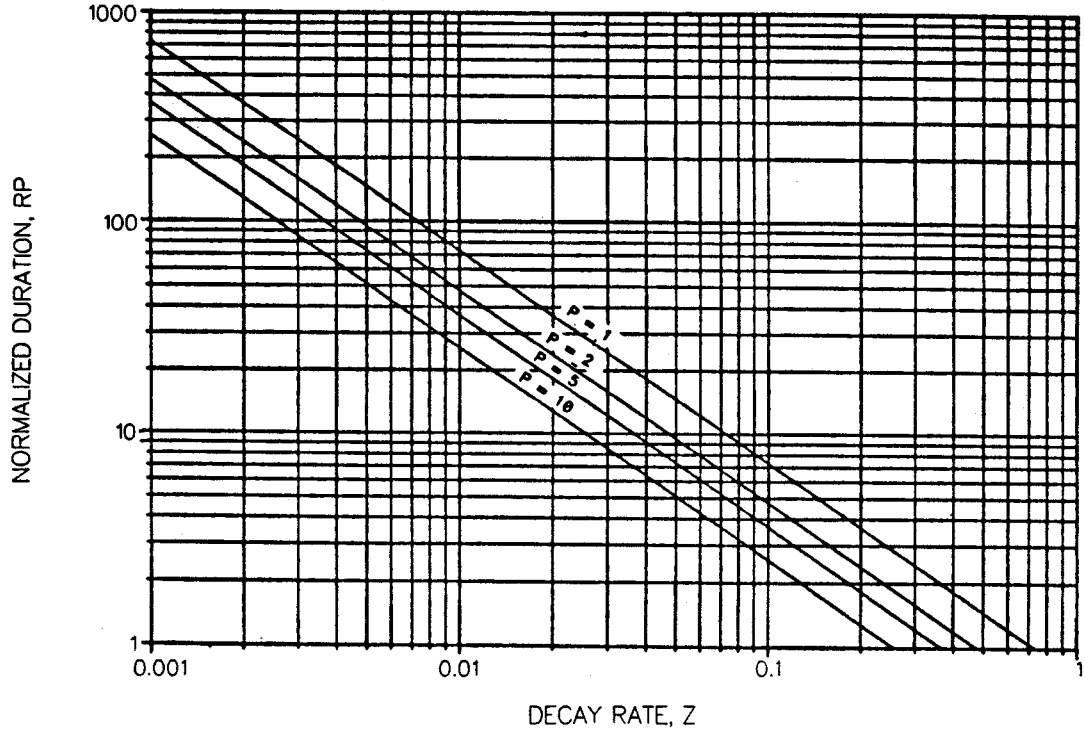

Figure 9 Normalized Duration (RP=TP/T) of a Decaying Sinusoid vs Decay Rate (Z) of a Decaying Sinusoid for Different Values of P.

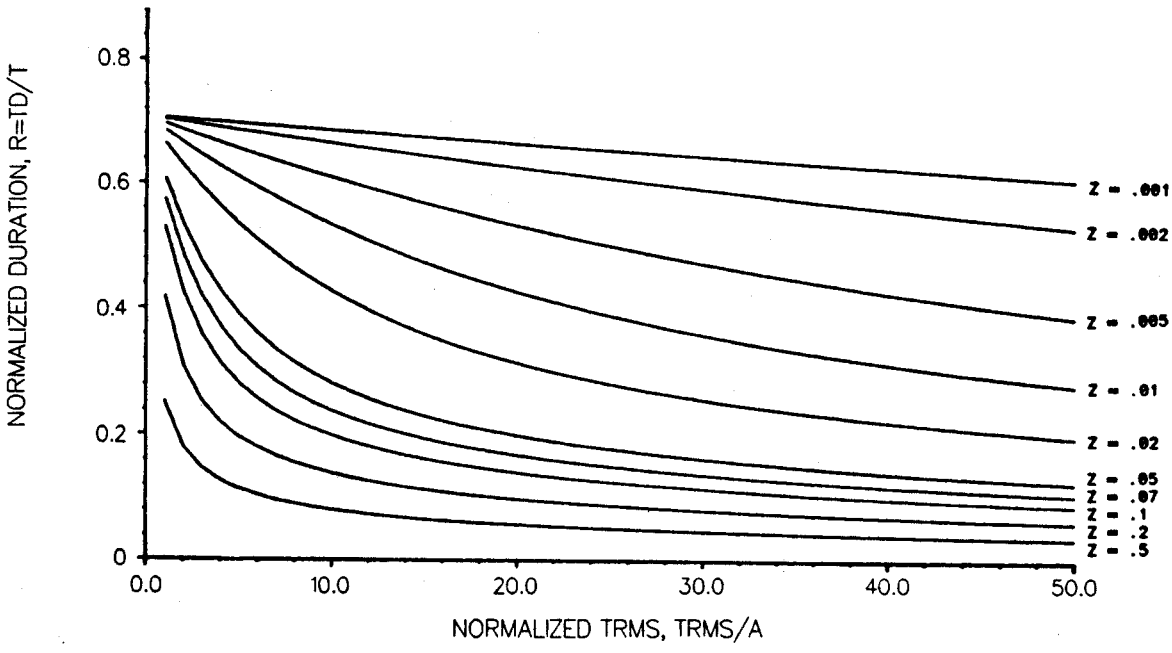

Figure 10 Normalized TRMS (TRMS/A) vs Normalized Duration (R=TD/T) at Different Decay Rates (Z) for a Decaying Sinusoid Pulse with Amplitude A, Period T, and Duration TD.

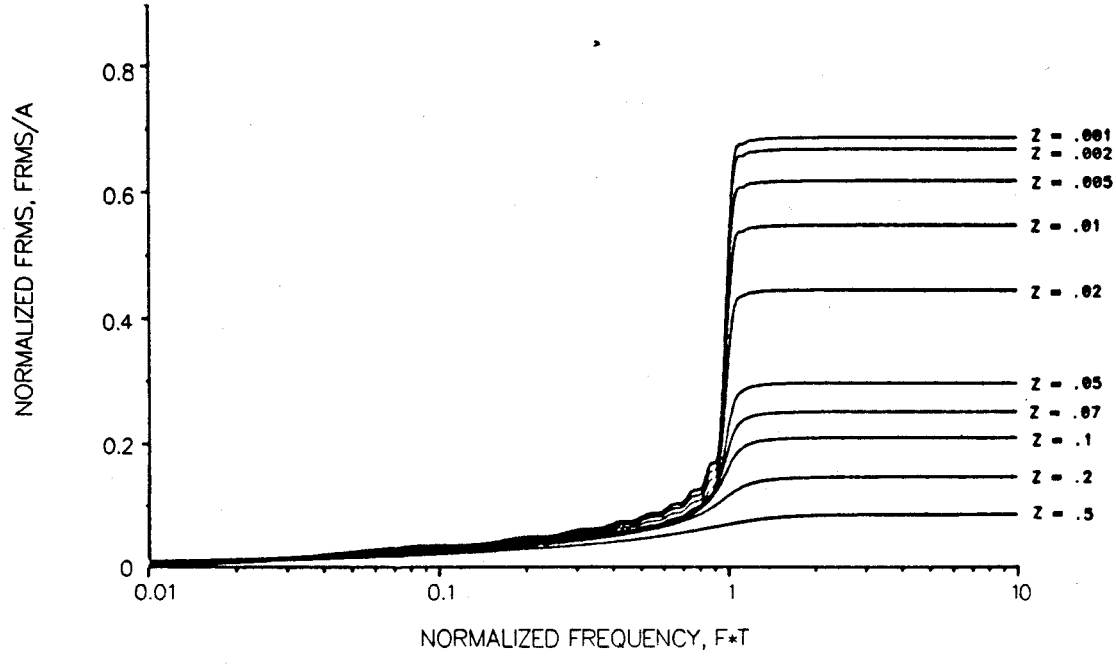

Figure 11 Normalized FRMS (FRMS/A) vs Normalized Frequency (F*T) at R=9 and at Various Decay Rates (Z) for a Decaying Sinusoid Pulse.

The frequency domain RMS for the decaying sinusoid pulse can be found by first solving Equation (4) analytically to get:

$$|\ddot{X}(f)| = \frac{AET}{4\pi}\left[C_1 \cos C_3 - \frac{C_1}{E} + C_2 \sin C_3 - D_1 \cos C_4 + \frac{D_1}{E} - D_2 \sin C_4\right] + j\left[\frac{AET}{4\pi} - C_1 \sin C_3 + C_2 \cos C_3 - \frac{C_2}{E} + D_1 \sin C_4 - D_2 \cos C_4 + \frac{D_2}{E}\right] \quad (11)$$

where,

$$C_1 = \frac{(fT - 1)}{(fT - 1)^2 + Z^2} \qquad C_2 = \frac{Z}{(fT - 1)^2 + Z^2}$$

$$C_3 = 2\pi R\,(fT-1) \qquad C_4 = 2\pi R\,(fT+1)$$

$$D_1 = \frac{(fT + 1)}{(fT - 1)^2 + Z^2} \qquad D_2 = \frac{Z}{(fT + 1)^2 + Z^2}$$

$$E = e^{-2\pi ZR}$$

and then solving Equation (3) numerically to produce a plot of normalized FRMS versus normalized frequency for a specified R value such as that shown in Figure 11 for various values of Z and R=9. The values of T, Z, and A are now determined for this decaying sinusoid component. The procedure is repeated if other components are necessary.

One final step in the definition of the entire decaying sinusoidal pulse is required if the peak acceleration of the test input is different from the peak acceleration of the field data. Should this be the case, the values of A are scaled by a constant factor so that the peak acceleration of the decaying sinusoid test pulse matches the peak acceleration of the field data.

Haversine Test Specification:

The duration of the haversine pulse is selected by taking TH as the period corresponding to the frequency below which all contributions to the overall RMS are made in the FRMS plot. If there is a single predominant frequency, F, in the FRMS plot, one would take TH as 1/F.

Once TH is selected, then the normalized duration for the haversine pulse can be calculated:

$$RH = \frac{TD}{TH} \quad (12)$$

Solving Equation (2) for a haversine pulse as defined in Equation (1), the following expression for normalized TRMSO versus RH is obtained:

$$\frac{TRMSO(RH)}{A} = \begin{cases} \frac{1}{2}\left[\frac{3}{2} + \frac{C_5}{\pi RH}\right]^{1/2}, & 0 < RH \le 1 \\ \frac{1}{2}\left[\frac{3}{2RH}\right]^{1/2}, & RH > 1 \end{cases} \quad (13)$$

where,

$$C_5 = \left(\frac{1}{8}\sin 4\pi RH - \sin 2\pi RH\right)$$

Figure 12 provides a plot of Equation (13) which can be used to find TRMSO(RH)/A for a given value of RH determined from Equation (12). The value of A necessary to match the TRMSO value from the field data can now be found by simple multiplication.

A normalized FRMS plot as a function of normalized frequency for various values of RH is given in Figure 13. This plot was generated by first finding the Fourier transform (Equation (4)) of the haversine pulse (Equation (1)):

$$|\ddot{X}(f)| = A \cdot K\,[\sin 2\pi fTH] + j\,A \cdot K\,[\cos 2\pi fTH - 1] \quad (14)$$

where,

$$K = \frac{1}{4\pi f}\left[\frac{1}{1 - (fTH)^2}\right]$$

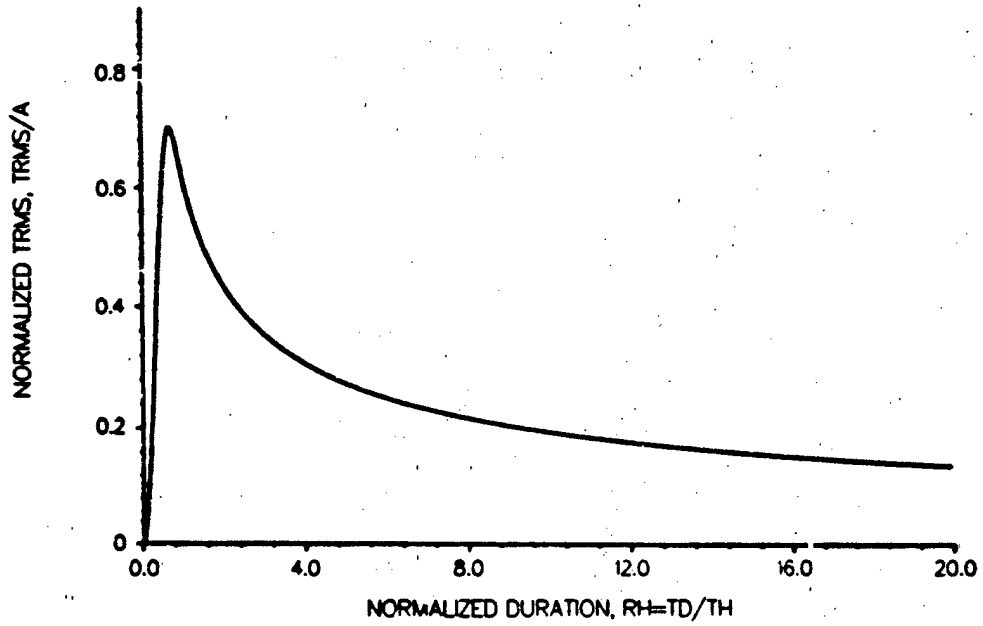

Figure 12 Normalized TRMS (TRMS/A) vs Normalized Duration (RH=TD/TH) for a Haversine Pulse with Amplitude (A) and Baseline Duration (TH). (TD = Duration of Input Time History.)

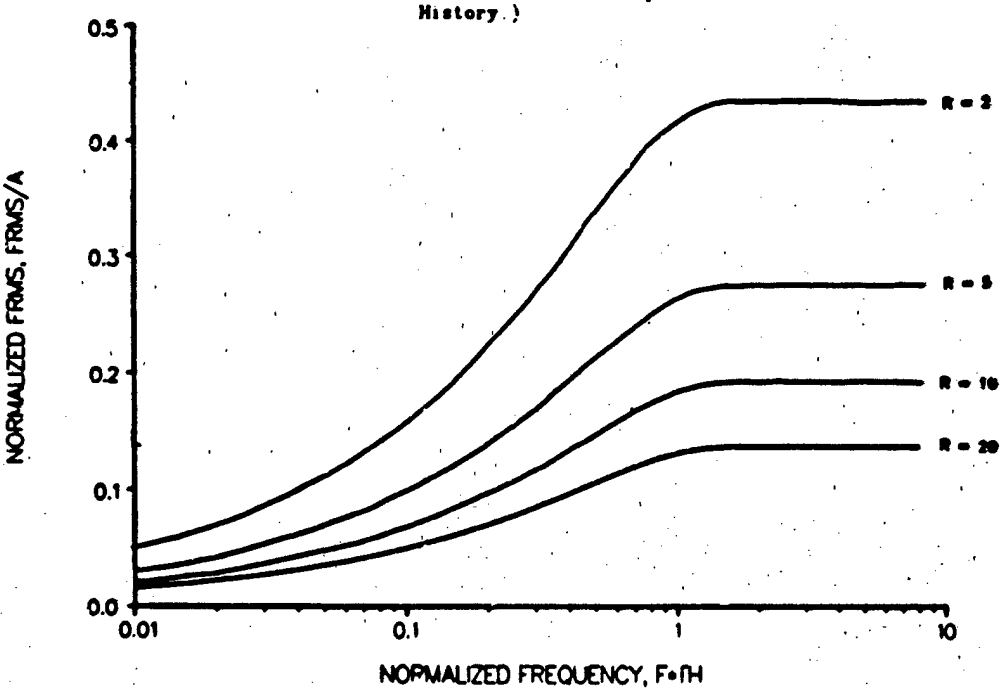

Figure 13 Normalized FRMS (FRMS/A) vs Normalized Frequency (F•TH) at Various RH Values (RH=TD/TH) for a Haversine Pulse with Amplitude (A) and Baseline Duration (TH). (TD = Duration of Input Time History.)

This result was then used in Equation (3) and the integration was carried out numerically.

A final modification to the value of A is necessary if the value determined by matching TRMSO differs from the peak value seen in the field data. The two peak values are made identical in this circumstance.

COMPARISON OF SHOCK TEST SPECIFICATION METHODS

A comparison of the shock test specification method introduced above and the standard method of shock spectrum enveloping was completed. The time history in Figure 1 was taken as the field data having the following parameters:

TRMSO = 108 g

TD = 0.006 s

T = 0.00067 s (1 / 1500 Hz)

TP = 0.0035 (P = 10)

MAXIMUM PEAK = 505 g

Three test specifications were evaluated and were denoted methods A, B, and C. Method A uses the proposed method without the final modification for the peak value. Method B includes the final modification for the peak value. Finally, Method C derives test inputs by shock spectrum enveloping. The test specifications are given in Table I. The resulting shock test inputs are shown in Figures 14 and 15. The corresponding shock characterizations are shown in Figures 16-19. For purposes of comparison with shock spectrum techniques, the shock spectra for the derived shock test inputs are shown in Figures 20a-c.

Two approaches were taken in judging the consistency of the three test specification methods. First, the shock characteristics in Table II were compiled for the shock inputs derived by each method. For ease of visualization, Figure 21 was created to show the shock input characteristics normalized with respect to the field data. Figure 21 shows that:

* Only Method B using a decaying sinusoid input is consistent in all categories.
* Method C generally produces conservative results except with regard to the maximum negative peak criterion.
* Methods A and B more closely match the field data than Method C in general.

Table I. Test Specifications for Methods A, B, and C.

	Shock Test Technique				
	Decaying Sinusoid*			Haversine	
Method**	A (g)	1/T (Hz)	Z	A (g)	TH (s)
A	432	1500	0.07	527	.00067
B	570	1500	0.07	505	.00067
C	296 1300	1550 4000	0.05 0.4	1300	.00033

* A compensating pulse must be added to ensure that the shaker displacement and velocity are zero at the end of the test (see Reference 10).

** Method A - Matched FRMS and TRMSO.
Method B - Method A modified to match maximum peak value.
Method C - Current method of shock spectrum enveloping.

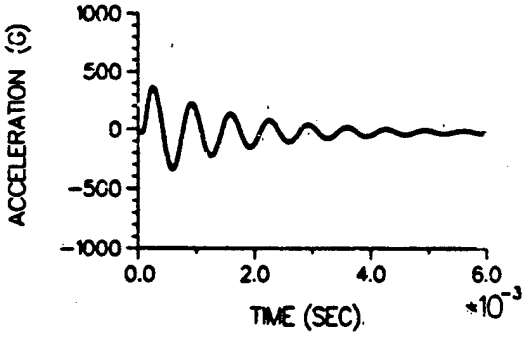

Figure 14a Test Input Derived by Method A Using Decaying Sinusoid Pulses (AD is designation in succeeding characterizations of this pulse).

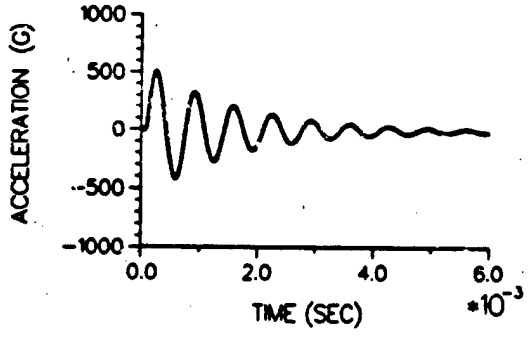

Figure 14b Test Input Derived by Method B Using Decaying Sinusoid Pulses (BD is designation in succeeding characterizations of this pulse).

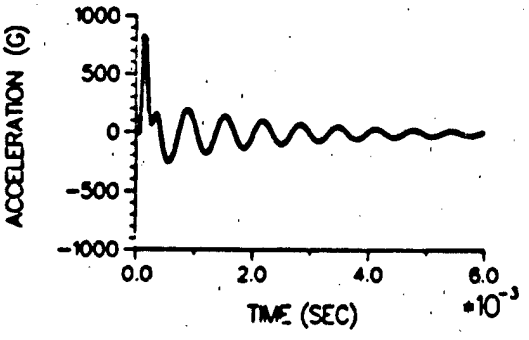

Figure 14c Test Input Derived by Method C Using Decaying Sinusoid Pulses (CD is designation in succeeding characterizations of this pulse).

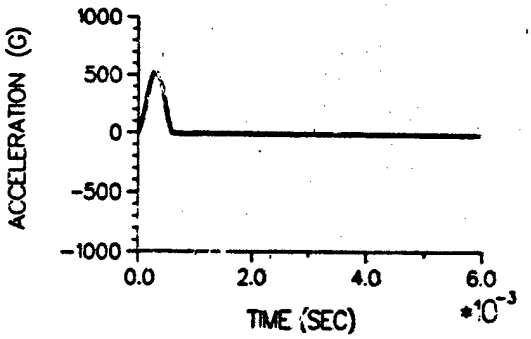

Figure 15a Test Input Derived by Method A Using a Haversine Pulse (AH is designation in succeeding characterizations of this pulse).

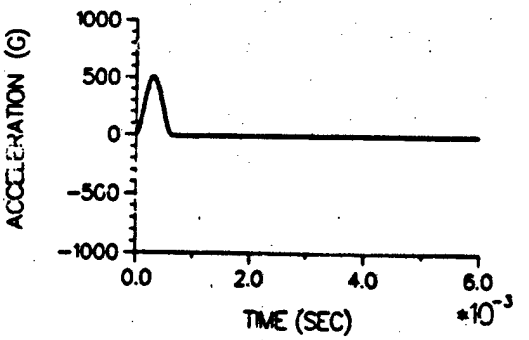

Figure 15b Test Input Derived by Method B Using a Haversine Pulse (BH is designation in succeeding characterizations of this pulse).

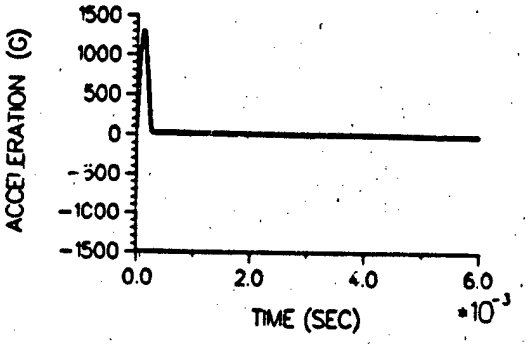

Figure 15c Test Input Derived by Method C Using a Haversine Pulse (CH is designation in succeeding characterizations of this pulse)

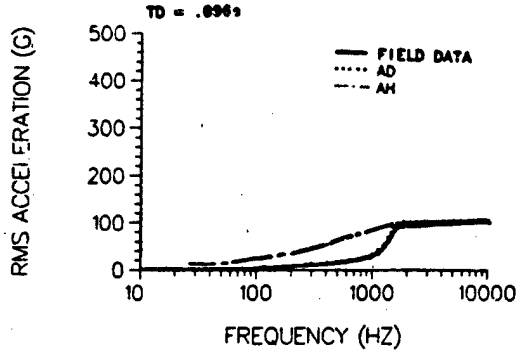

Figure 16a RMS Acceleration vs Frequency Comparison between Field Data and Method A Test Inputs.

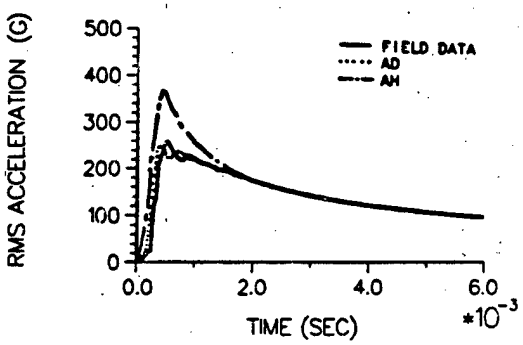

Figure 17a RMS Acceleration vs Time Comparison between Field Data and Method A Test Inputs.

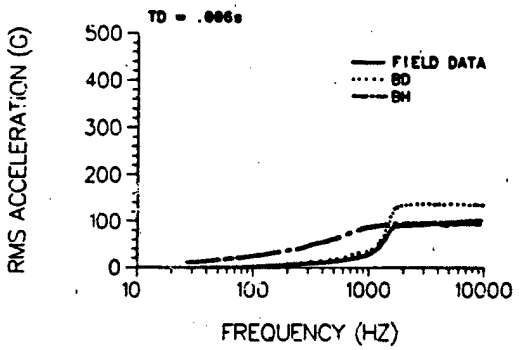

Figure 16b RMS Acceleration vs Frequency Comparison between Field Data and Method B Test Inputs.

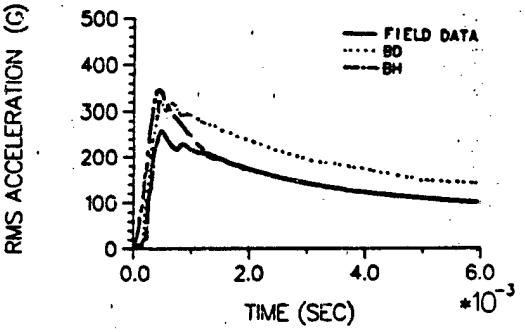

Figure 17b RMS Acceleration vs Time Comparison between Field Data and Method B Test Inputs.

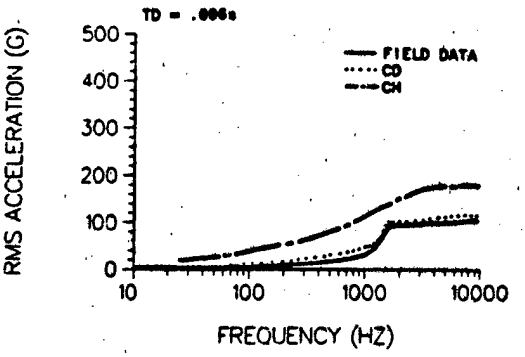

Figure 16c RMS Acceleration vs Frequency Comparison between Field Data and Method C Test Inputs.

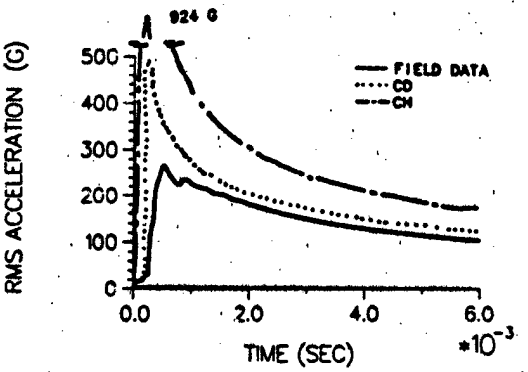

Figure 17c RMS Acceleration vs Time Comparison between Field Data and Method C Test Inputs.

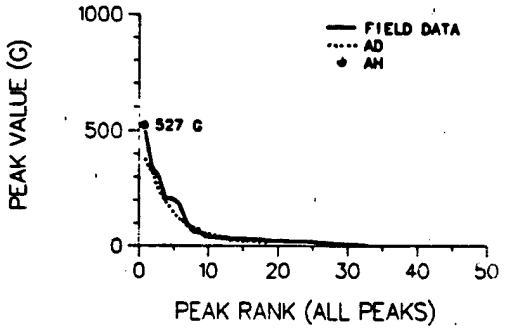

Figure 18a Ranked Absolute Peak Value Comparison between Field Data and Method A Test Inputs.

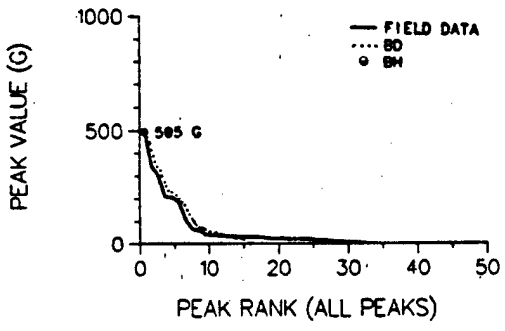

Figure 18b Ranked Absolute Peak Value Comparison between Field Data and Method B Test Inputs.

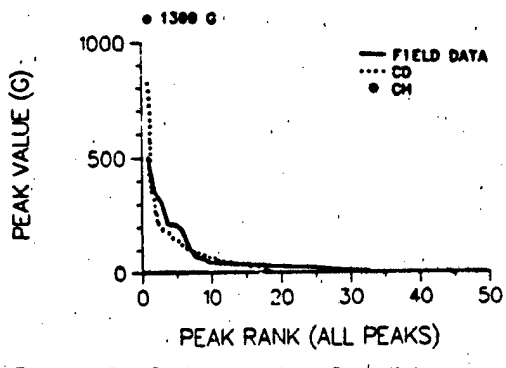

Figure 18c Ranked Absolute Peak Value Comparison between Field Data and Method C Test Inputs.

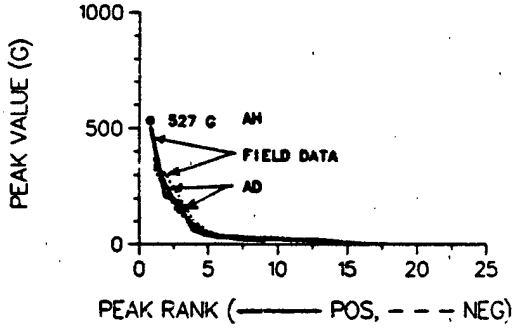

Figure 19a Ranked Positive and Negative Peak Value Comparison between Field Data and Method A Test Inputs.

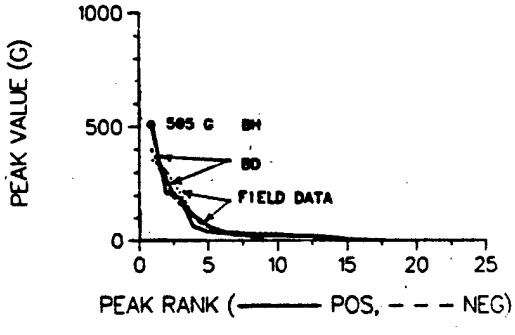

Figure 19b Ranked Positive and Negative Peak Value Comparison between Field Data and Method B Test Inputs.

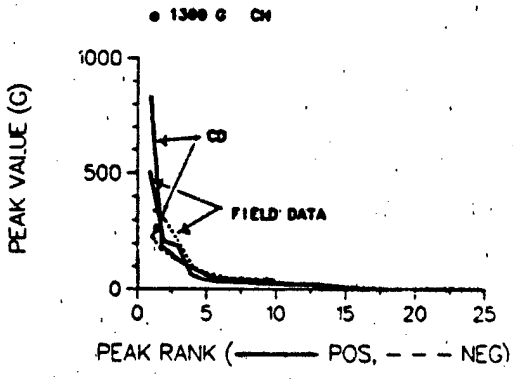

Figure 19c Ranked Positive and Negative Peak Value Comparison between Field Data and Method C Test Inputs.

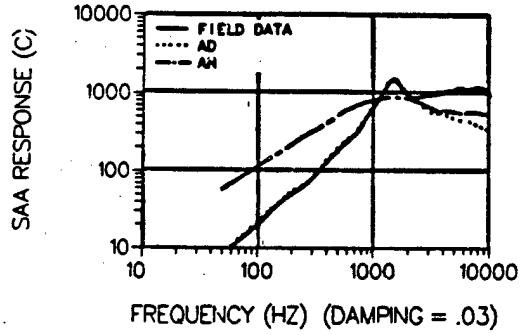

Figure 20a Shock Spectrum Comparison between Field Data and Method A Test Inputs.

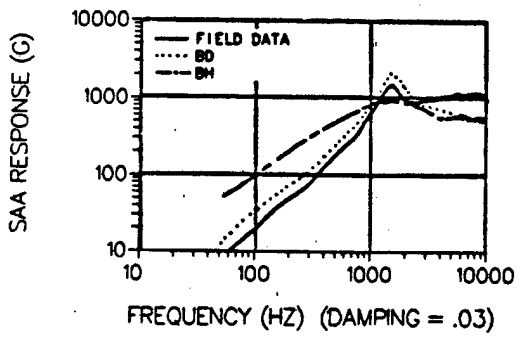

Figure 20b Shock Spectrum Comparison between Field Data and Method B Test Inputs.

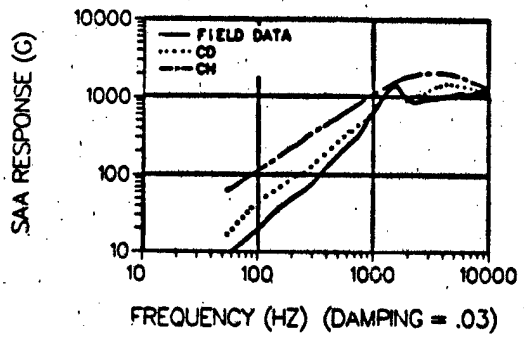

Figure 20c Shock Spectrum Comparison between Field Data and Method C Test Inputs.

Table 11. Comparison of Shock Input Characteristics (TD = .006s).

Test Spec Method*	Shock Excitation	Shock Characteristics			
		TRMSO (g)	Max Peak (g)	Max Positive Peak (g)	Max Negative Peak (g)
—	Field Data	108	505	505	352
A	Decaying Sinusoid (AD)	108	383	383	315
	Haversine (AH)	108	527	527	0
B	Decaying Sinusoid (BD)	142	505	505	416
	Haversine (BH)	104	505	505	0
C	Decaying Sinusoid (CD)	121	822	822	250
	Haversine (CH)	178	1300	1300	0

* Method A – Matched FRMS and TRMSO.
Method B – Method A modified to match maximum peak value.
Method C – Current method of shock spectrum enveloping.

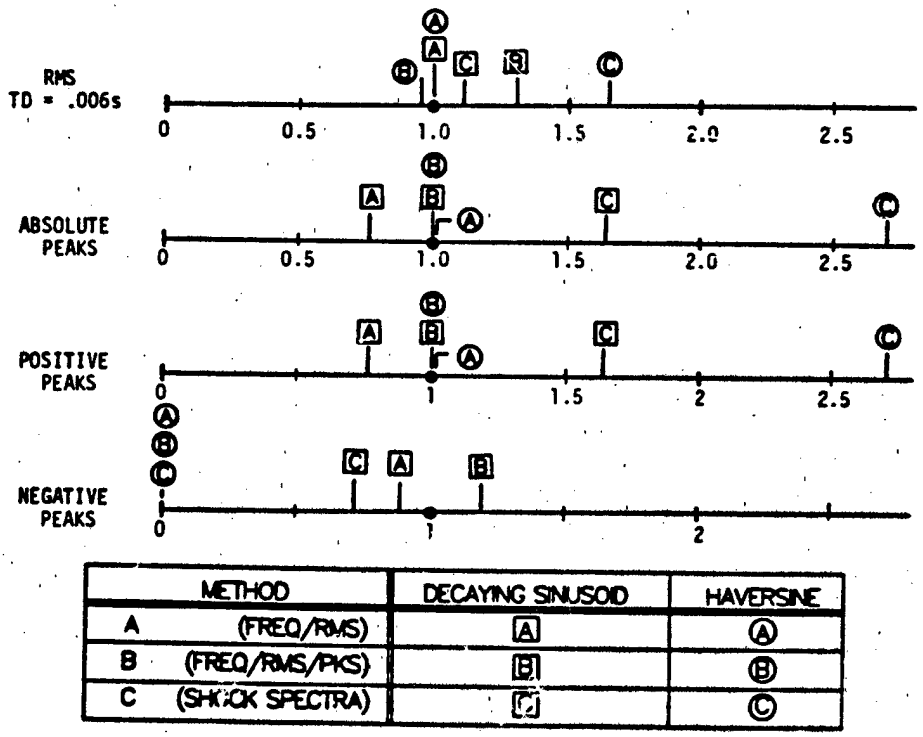

Figure 21 Normalized Shock Input Characterization. (Test Specification Value / Field Data Value).

Table III. Comparison of Shock Response Characteristics (TD = .035s).

Test Spec Method*	Shock Excitation	Shock Characteristics: TRMSO (g)	Max Peak (g)	Max Positive Peak (g)	Max Negative Peak (g)
—	Field Data	60	242	242	185
A	Decaying Sinusoid (AD)	70	232	232	165
	Haversine (AH)	242	463	463	448
B	Decaying Sinusoid (BD)	92	306	306	218
	Haversine (BH)	231	442	442	428
C	Decaying Sinusoid (CD)	112	301	257	301
	Haversine (CH)	274	521	521	505

* Method A - Matched FRMS and TRMSO.
Method B - Method A modified to match maximum peak value.
Method C - Current method of shock spectrum enveloping.

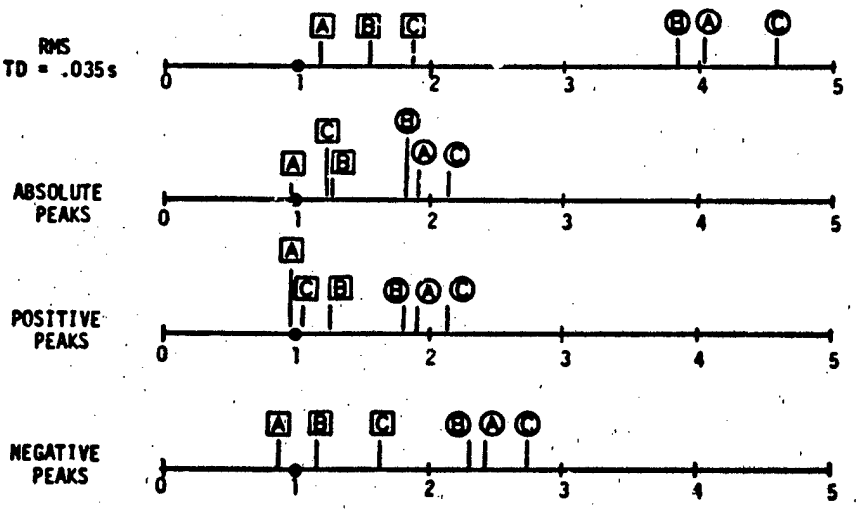

METHOD		DECAYING SINUSOID	HAVERSINE
A	(FREQ/RMS)	A	Ⓐ
B	(FREQ/RMS/PKS)	B	Ⓑ
C	(SHOCK SPECTRA)	C	Ⓒ

Figure 22 Normalized Model Response Characterization (Test Model Response Value / Field Data Model Response Value).

As a second means of judging the consistency of the shock test inputs with the field data, each input was used to excite a MSC/NASTRAN model of a ~12.7cm (5 inch) long cantilever beam. Response time histories at the end of the beam model as well as shock characterizations are shown in the Appendix. These data are summarized in Table III and Figure 22, and correspond to the data in Table II and Figure 21. The main observations from these data are that:

* All methods are consistent in being higher than the field data except Method A which produces response peaks slightly lower than the field data.

* Responses produced by haversine inputs are always higher than those produced by decaying sinusoid inputs.

CONCLUSIONS

A new method of specifying decaying sinusoid and haversine shock tests has been developed and demonstrated. The method is based on the more complete characterization of both field and laboratory shock environments. These shock characterizations include time and frequency domain RMS acceleration and ranked acceleration peaks. These characterizations are shown to be very useful alternatives to shock spectrum characterizations which fail to retain valuable information about the field shock time history. Such information is essential if the field shock environment is to be simulated to the greatest extent possible in the shock laboratory.

Decaying sinusoidal shock tests specified according to the proposed method are found to produce both shock test inputs and responses which are consistent with actual field shock data. This claim cannot be made by the single shock test inputs produced by the standard method of shock test specification based on shock spectrum enveloping. The characterizations in this paper show that decaying sinusoidal shock test inputs may be below field environment levels while those produced using haversines may be considerably higher. The degree of conservatism associated with all of these test specification needs to be studied in more detail. The methods of Reference 6 provide the basis for this type of analysis.

REFERENCES

1. Biot, M. A., "Theory of Elastic Systems Vibrating Under Transient Impulse with an Application to Earthquake-Proof Buildings," Proceedings of the National Academy of Science, Vol. 19, No. 2, 1933, pp. 262-268.

2. Biot, M. A., "A Mechanical Analyzer for the Prediction of Earthquake Stresses," Bulletin of the Seismological Society of America," Vol. 31, 1941, pp. 151-171.

3. Rader, W. P., and W. F. Bang, "A Summary of Pyrotechnic Shock in the Aerospace Industry," Shock and Vibration Bulletin, Vol. 41, Part 5, 1970, pp. 9-15.

4. Kelly, R. D., and G. Richman, Principles and Techniques of Shock Data Analysis, The Shock and Vibration Information Center, USDOD, SVM-5, 1969.

5. Smallwood, D. O., "Time History Synthesis for Shock Testing on Shakers," Seminar on Understanding Digital Control and Analysis in Vibration Test Systems, Greenbelt, Maryland, June 1975, pp. 23-41.

6. Baca, T. J., "Characterization of Conservatism in Mechanical Shock Testing of Structures," Ph.D. Dissertation, Department of Civil Engineering, Stanford University, September 1982.

7. Spanos, P-T, D., "Digital Synthesis of Response-Design Spectrum Compatible Earthquake Records for Dynamic Analyses," The Shock and Vibration Digest, Vol. 15, No. 3, March 1983, pp. 21-30.

8. Baca, T. J., "Evaluation and Control of Conservatism in Drop Table Shock Tests," Shock and Vibration Bulletin, Vol. 53, Part 1, 1983, pp. 163-176.

9. Cooley, J. W., and J. W. Tukey, "An Algorithm for the Machine Calculation of Complex Fourier Series," Mathematics of Computation, Vol. 19, April 1965, pp. 297-301.

10. Smallwood, D. O., and A. R. Nord, "Matching Shock Spectra with Sums of Decaying Sinusoids Compensated for Shaker Velocity and Displacement Limitations," Shock and Vibration Bulletin, Vol. 44, Part 3, 1974, pp. 43-56.

APPENDIX

This appendix includes the time histories and response characterizations which were calculated using a MSC/NASTRAN finite element model of a 12.7 cm (5 inch) long cantilever beam excited by the test inputs derived from all three test specifications techniques using decaying sinusoid and haversine inputs. The responses are calculated at the free end of the beam.

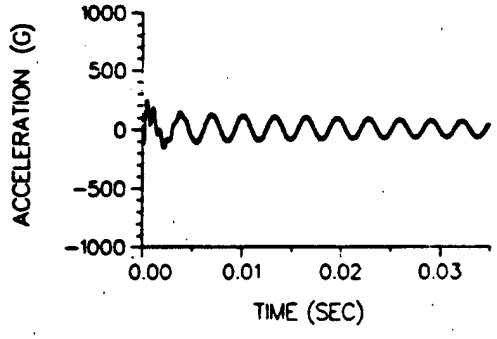

Figure A1a Calculated Model Response from Test Input Derived by Method A Using Decaying Sinusoid Pulses (AD).

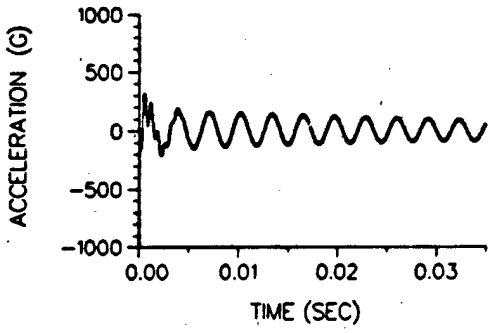

Figure A1b Calculated Model Response from Test Input Derived by Method B Using Decaying Sinusoid Pulses (BD).

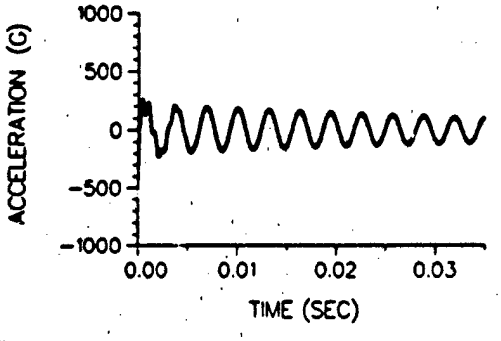

Figure A1c Calculated Model Response from Test Input Derived by Method C Using Decaying Sinusoid Pulses (CD)

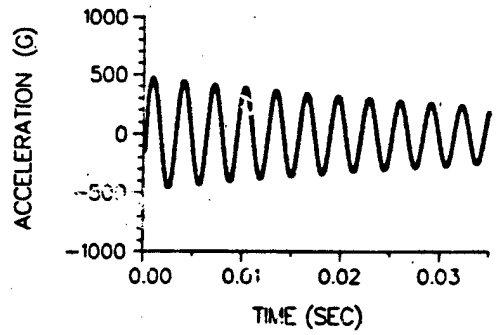

Figure A2a Calculated Model Response from Test Input Derived by Method A Using a Haversine Pulse (AH).

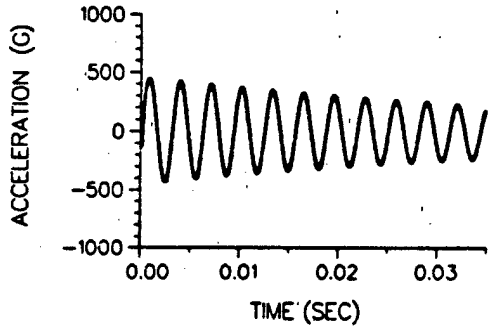

Figure A2b Calculated Model Responre from Test Input Derived by Method B Using a Haversine Pulse (BH).

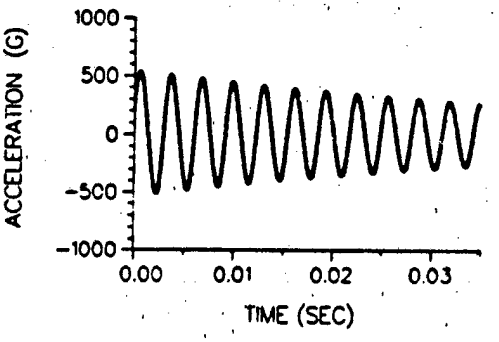

Figure A2c Calculated Model Response from Test Input Derived by Method C Using a Haversine Pulse (CH).

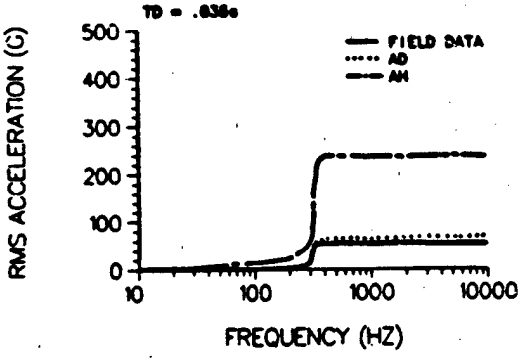

Figure A3a RMS Acceleration vs Frequency Comparison between Field Data and Method A Test Responses (Model Calculations).

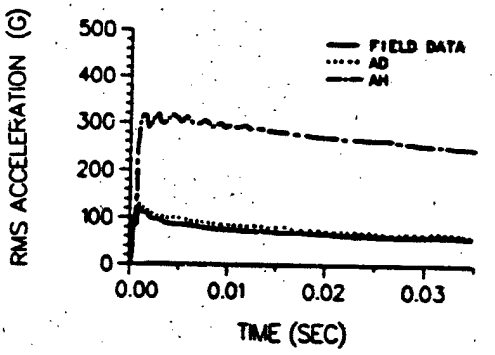

Figure A4a RMS Acceleration vs Time Comparison between Field Data and Method A Test Responses (Model Calculations).

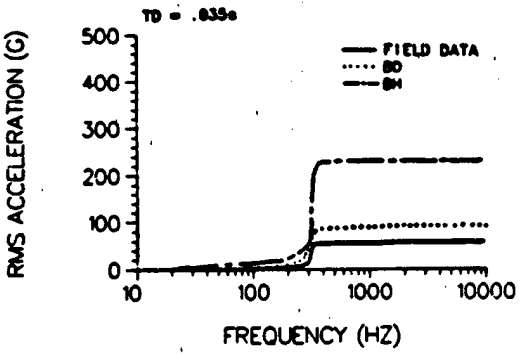

Figure A3b RMS Acceleration vs Frequency Comparison between Field Data and Method B Test Responses (Model Calculations).

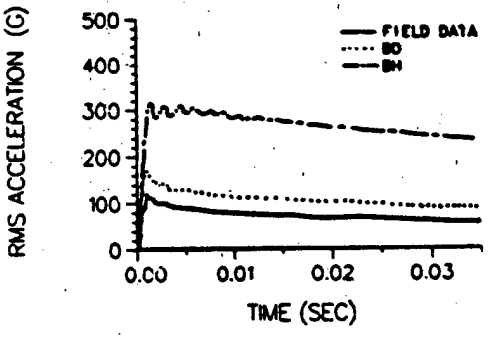

Figure A4b RMS Acceleration vs Time Comparison between Field Data and Method B Test Responses (Model Calculations).

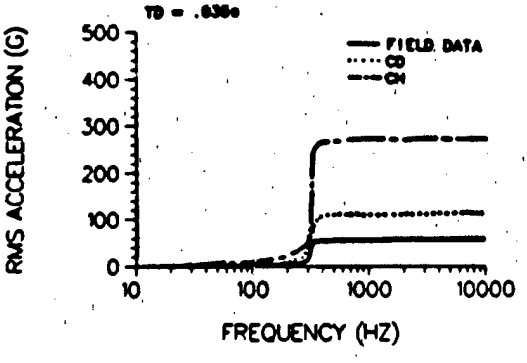

Figure A3c RMS Acceleration vs Frequency Comparison between Field Data and Method C Test Responses (Model Calculations).

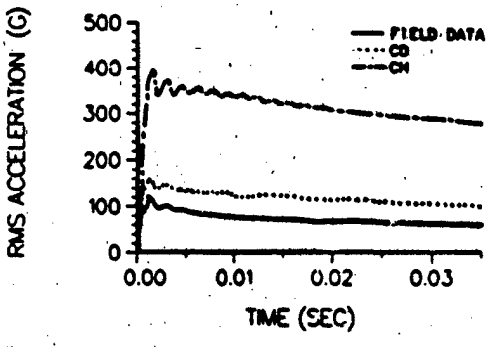

Figure A4c RMS Acceleration vs Time Comparison between Field Data and Method C Test Responses (Model Calculations).

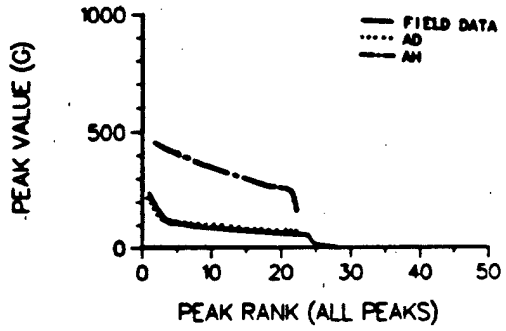

Figure A5a Ranked Absolute Peak Value Comparison between Field Data and Method A Test Responses (Model Calculation).

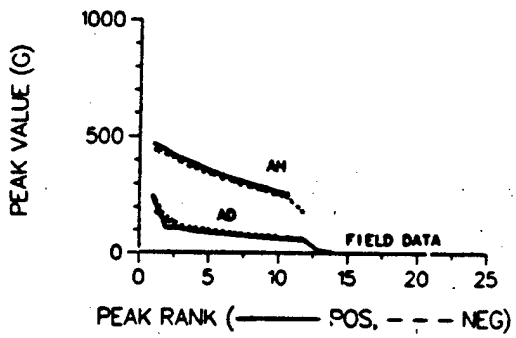

Figure A6a Ranked Positive and Negative Peak Value Comparison between Field Data and Method A Test Responses (Model Calculation).

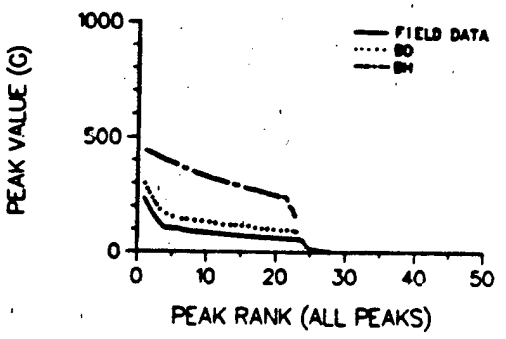

Figure A5b Ranked Absolute Peak Value Comparison between Field Data and Method B Test Responses (Model Calculation).

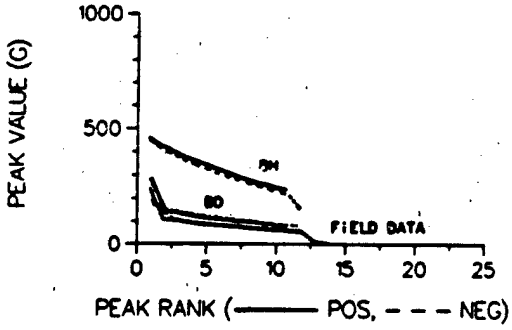

Figure A6b Ranked Positive and Negative Peak Value Comparison between Field Data and Method B Test Responses (Model Calculation).

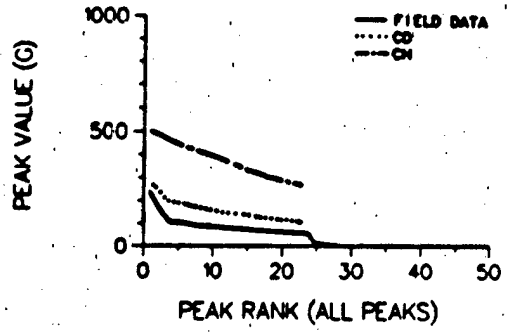

Figure A5c Ranked Absolute Peak Value Comparison between Field Data and Method C Test Responses (Model Calculation).

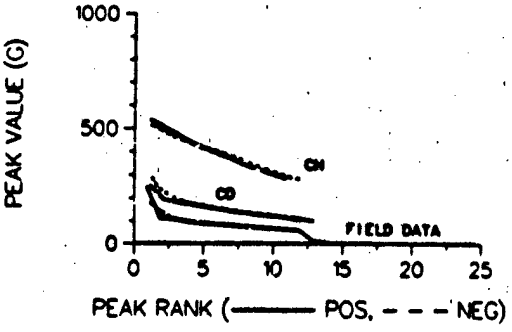

Figure A6c Ranked Positive and Negative Peak Value Comparison between Field Data and Method C Test Responses (Model Calculation).

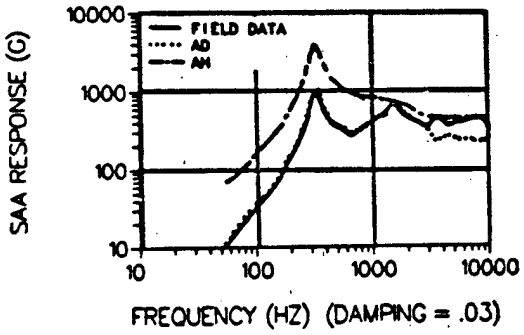

Figure A7a Shock Spectrum Comparison between Field Data and Method A Test Responses (Model Calculation).

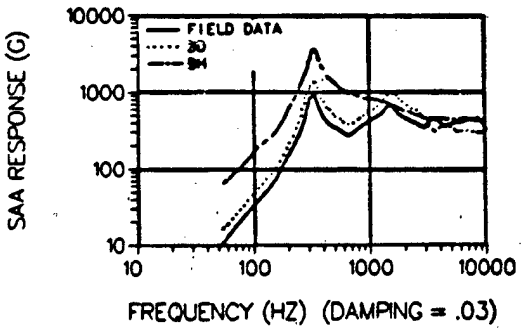

Figure A7b Shock Spectrum Comparison between Field Data and Method B Test Responses (Model Calculation).

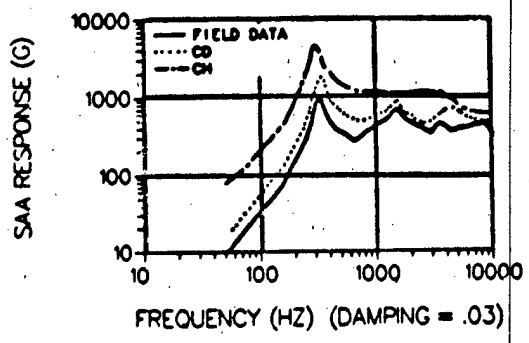

Figure A7c Shock Spectrum Comparison between Field Data and Method C Test Responses (Model Calculation).

DISCUSSION

Mr. Strauss (Rocketdyne): Does it apply primarily to shock or transient pulses that are primarily a single frequency? Many times transient pulses have a broad band frequency content.

Mr. Baca: No, it can be applied for multiple frequencies. The example I showed was for one frequency for simplicity, but it is possible to pick out which frequencies are making the contributions to the overall rms level.

Mr. Strauss: Would you then apply multiple decaying sinusoids superimposed on each other?

Mr. Baca: Yes. Currently, when we synthesize a decaying sinusoid pulse, we are selecting different sinusoidal components to match the peaks in our shock spectra. I would match this particular frequency where I see significant energy applied in field data.

Mr. Strauss: One of the papers this morning addressed some overtest and undertest problems by using decaying sinusoids, or shaker type tests, as opposed to pyrotechnic devices which are the real source. Have you compared the different kinds of results from actual test cases on hardware?

Mr. Baca: We are currently gathering data, and we are applying both this method and the shock spectra to try to come up with some kind of an evaluation.

Mr. Geers (Lockheed): I assume the field data in these comparisons looked more like a decaying sinusoid than a haversine. Is that right?

Mr. Baca: That first plot is field data.

Mr. Geers: That is why the decaying sinusoid looked much better in this case. You have to look at the nature of the field data and make a judgment as to whether you will take a single pulse type representation or a decaying sinusoid. Is that right?

Mr. Baca: In my experience the decision is often made for you. First of all, you do have that judgement to make just because you know it is a pyrotechnic type shock versus maybe a transportation shock which has that one-sided nature, or maybe a blast shock. Even though we would like to use a decaying sinusoidal pulse, many times the G levels are such that we cannot reach that on a shaker. So, we are forced to go to a drop table type technique just to reach some of the G levels we are concerned about. That is why I feel it is important to at least address the issue of how to specify a test using the simple pulses, even though you know that is not the best way to do it.

Mr. Geers: But you try to do the best with what you have.